Synthesis and evaluation of functional carboxylic acid based poly(ϵCL-st-αCOOHϵCL)-b-PEG-b-poly(ϵCL-st-αCOOHϵCL) copolymers for neodymium and cerium complexation

Loona Ferrie, Carlos Arrambide, Vincent Darcos, Benedicte Prelot, Sophie Monge

Synthesis and evaluation of functional carboxylic acid based poly(εCL-*st*-αCOOHεCL)-*b*-PEG-*b*-poly(εCL-*st*-αCOOHεCL) copolymers for neodymium and cerium complexation

Loona Ferrie[a], Carlos Arrambide Cruz[b], Vincent Darcos[b,**], Benedicte Prelot[a], Sophie Monge[a,*]

[a] ICGM, Univ. Montpellier, CNRS, ENSCM, Montpellier, France

[b] IBMM, Univ. Montpellier, CNRS, ENSCM, Montpellier, France

Corresponding authors

E-mail addresses:

* sophie.monge-darcos@umontpellier.fr

** vincent.darcos@umontpellier.fr

Abstract

Original carboxylic acid-based copolymers have been developed for the complexation of actinides. For such purpose, ring-opening copolymerizations of α-benzyl carboxylate-ε-caprolactone (BzCL) and ε-caprolactone (εCL) have been carried out with poly(ethylene glycol) (PEG) as macro-initiator and tin(II) octanoate, as catalyst, to afford poly(εCL-*st*-αBzεCL)-*b*-PEG-*b*-poly(εCL-*st*-αBzεCL) (PB) copolymers. Three different εCL/BzCL ratios were targeted (90/10, 75/25 and 50/50), leading to $PB_{10\%}$, $PB_{25\%}$ and $PB_{50\%}$, respectively. Then, hydrogenation of the prepared copolymers allowed the deprotection of benzyl esters to carboxylic acids groups, leading to poly(εCL-*st*-αCOOHεCL)-*b*-PEG-*b*-poly(εCL-*st*-αCOOHεCL) copolymers ($PA_{10\%}$, $PA_{25\%}$ and $PA_{50\%}$). All materials were fully characterized by ^{1}H NMR, ^{13}C NMR and size exclusion chromatography. Experimental ratios were found to be close from theoretical ones as equal to 92/08, 75/25, and 60/40. Molecular weight was the same for all copolymers (4000 $g.mol^{-1}$). Complexing properties of the different copolymers were studied by Isothermal Titration Calorimetry (ITC) with neodymium (Nd(III)) and cerium (Ce(III)), used as actinide surrogates. ITC enabled the determination of the full thermodynamic profile (ΔG, ΔH, TΔS, Ka, and stoichiometry). The results showed that $PA_{25\%}$ was the polymer with the highest sorption capacity (13.6 $mg.g^{-1}$ for Nd(III) and 13.7 $mg.g^{-1}$ for Ce(III)) and the highest binding constant (8500 M^{-1} and 5500 M^{-1} for Nd(III) and Ce(III), respectively). This demonstrated that by increasing the amount of complexing carboxylic acid functions, the complexing capacity did not necessarily increase as well, reaching a maximum with $PA_{25\%}$. In a more general manner, all developed copolymers are very promising for cation complexation.

Keywords: ε-caprolactone, poly(ethylene glycol), carboxylic acid, complexation, ITC, cerium, neodymium

1. Introduction

Actinides are elements widely used in various domains such as nuclear industry in power plants [1, 2], military field with atomic bombs, dirty bombs [3-5] or other armament [6], in medicine field [7, 8], etc. Unfortunately, their radioactivity makes them extremely toxic. Thus, research on the removal of actinides by complexation is of sustained interest in order to develop efficient strategies during accidents and contamination, whether physical or environmental. Particularly, bodily contaminations can be either external (contamination of healthy skin) and/or internal (contamination of organs and tissues), due to the consumption of water or radioactive food, inhalation of contaminated air or skin contact with radioactive elements [9]. During internal contamination, actinides accumulate in target organs (liver, kidneys) and tissues, causing serious damage to health of affected people [10]. When these elements have accumulated in the body, they can notably lead to the failure and destruction of bone marrow cells [11, 12], fertility problems [13], multiple cancers [14], and finally death of the contaminated person. By external body contact, actinides cause skin burns and may penetrate the skin barrier after only few hours [15].

Nowadays, internal or external body decontamination can be treated using specific compounds, in particular low-molecular weight organic molecules bearing appropriate chelating groups [16, 17] which complex actinides, allowing their elimination from the contaminated environment. For such purpose, to date, the main developed complexing functions reported in the literature were phosphonic [18, 19] and carboxylic [20, 21] acids. Currently, the main molecule used for body decontamination is a polyaminocarboxylic acid, namely the diethylenetriamine pentaacetic acid (DTPA) [22, 23]. This ligand, containing amino and carboxylic acid groups, proved to possess a high affinity for lanthanides and actinides, and was particular used for the complexation of internalized plutonium and americium. Side to DTPA, tetracetic acid derivatives (EDTA, CDTA, PDTA) were employed for the complexation of Cm(III) [24]. Other molecules carrying carboxylic acid functions were also developed for the complexation of actinides, demonstrating a great capacity for sorption and removal of these elements. For instance, diacylated diethylene triamines mixed with carboxylic acid fractions were synthesized to extract neodymium, a lanthanide used as a surrogate of actinides [25], and different carboxylic acids (acetic, glycolic, malonic) were studied for the complexation of

americium and curium [26, 27]. Malonic acid was also considered to complex neptunium [28] whereas glycolic acid was efficiently used in the case of thorium [29]. Hydroxycarboxylic acids allowed the decontamination of uranium [20], showing good properties for the extraction of this element from different surfaces. Anions of citrate also allowed the complexation of Nd(III) and Am(III) [30].

Side to low-molecular weight molecules, hydroxycarboxylic acid-based macromolecular structures were employed as complexing agents, in particular humic acids (HA), which contain a large number of functionalities, mainly carboxylic acids. HA proved to be of interest for the complexation of actinides [31-34], with possible selectivity [35]. Humic substances can form strong complexes with actinides thanks to strong metal-ligand interactions, and can act as both a complexant and a redox agent [36]. They were successfully employed for the complexation of actinides (IV) (Th, U, Pu) [37], or actinides (III) (Pu [38], Am [39]). However, complex chemical structure of humic acid makes them difficult to use and study. As a consequence, synthetic organic materials bearing many carboxylic acid functions with controllable properties that can be easily studied were developed. Even if lots of synthetic polymers were prepared for the sorption of metallic cations [40], only very limited examples of carboxylic acid-based water-soluble synthetic polymers were reported in the literature for the complexation of actinides. Polyacrylic acid (PAA) was used for the sorption of uranium [41]. Polyacrylate was also considered for the sorption of Cm(III) [42]. Another example of macromolecular systems containing carboxylic acids for the complexation of actinides dealt the use of functionalized calixarenes. Indeed, calix[4]arene carboxylic acid were studied for the complexation of neodymium, still used as a surrogate of actinides [43]. The calixarenes resulted from progressive substitution of the phenolic hydrogens of p-tert-butylcalix[4]arene by carboxylic acid functions [44]. The binding abilities of a series of ionizable calixarenes towards Th(IV) have notably been established by potentiometric measurements. Although the systems reported in the literature show interesting complexation capacities, it is worth developing new materials, in particular biocompatible, showing good extraction of actinides that could be usable for external/internal decontamination, for instance.

In the present contribution, the synthesis of original water-soluble copolymers carrying carboxylic acid complexing functions, based on poly(ε-caprolactone) (PCL) and poly(ethylene glycol) (PEG) is reported. Poly(ε-caprolactone) is a biocompatible

and biodegradable (with a slow kinetic) aliphatic polyester approved by the Food and Drug Administration (FDA) for skin and internal applications [45]. The combination of this polymer with PEG will lead to water-soluble materials (thus favouring rapid actinide sorption) and will allow modulating degradability of the final material (by making it faster) [46]. It is important to mention that PEG is a biocompatible polymer, widely used in many biomedical and pharmaceutical applications [47]. Numerous studies described the synthesis of poly(ε-caprolactone)-*b*-poly(ethylene glycol)-*b*-poly(ε-caprolactone) (PCL-*b*-PEG-*b*-PCL) copolymers for uses in the medical field, and in particular for drug administration [48-50], such as delivery of anti-cancer agents [51-53] or in tissue engineering [45, 54]. Polymers reported in this study are functionalized PCL-*b*-PEG-*b*-PCL copolymers, with PCLs containing a controlled ratio of pendant carboxylic acid groups equal to 10, 25, and 50%, namely poly(εCL-*st*-αCOOHεCL)-*b*-PEG-*b*-poly(εCL-*st*-αCOOHεCL), abbreviated $PA_{10\%}$, $PA_{25\%}$, $PA_{50\%}$, respectively. These materials allowed studying the influence of the acid groups rate on the complexation properties. The complexation study was carried out by Isothermal Titration Calorimetry (ITC) with neodymium (Nd(III)) and cerium (Ce(III)) as surrogates for actinides, in order to obtain the thermodynamic parameters of the different systems developed. The originality of the reported work in this contribution is that the actinide sequestrating materials developed were prepared from biocompatible moieties, allowing their consideration for decontamination application, where the use of functional polymers is nowadays still rare.

2. Experimental section

2.1. Materials

Lithium diisoproprylamide (2.0 M in THF/heptane/ethylbenzene, Sigma Aldrich), tin(II) 2-ethylhexanoate (Sigma Aldrich), palladium on carbon (10 wt.% loading, matrix activated, Sigma Aldrich), benzyl chloroformate (95%, stab. with ca 0.1% sodium carbonate, Alfa Aesar), neodymium(III) nitrate hexahydrate ($Nd(NO_3)_3.6H_2O$, Sigma Aldrich) and cerium(III) nitrate hexahydrate ($Ce(NO_3)_3.6H_2O$, Sigma Aldrich) were used without further purification. ε-Caprolactone (97 %, Sigma Aldrich) and toluene (Sigma Aldrich) were dried over calcium hydride for 24 hours at room temperature and distilled under reduce pressure. Poly(ethylene glycol (M_n = 2000 $g.mol^{-1}$, Sigma

Aldrich) was dried by azeotropic distillation with toluene. Dichloromethane, THF and ethyl acetate were purchased from Sigma Aldrich, were organic synthesis grade and used as received. Aqueous solutions for titration calorimetry were prepared using Milli-Q water of 18.2 MΩ.cm.

2.2. Analytical techniques

^{1}H and ^{13}C NMR analyzes were recorded with Bruker Avance III HD - 400 MHz, using $CDCl_3$ as deuterated solvent. For ^{1}H and ^{13}C NMR spectra, chemical shifts were referenced to the peak at 7.26 and 77.16 ppm, corresponding to the residual non-deuterated solvent and the carbon atom for $CDCl_3$, respectively.

Size exclusion chromatography (SEC) was performed using Varian 390-LC equipped with a RI refractive index detector. PLGel 5µm mixed-D column was used at 30 °C with a flow rate of 0.8 $mL.min^{-1}$ and THF as elution solvent. Linear poly(methyl methacrylate)s (PMMA) were used as standards.

FTIR spectroscopic studies were recorded with a Perkin-Elmer Spectrum 100 spectrometer equipped with an attenuated total reflectance (ATR) crystal (ZnSe). The wavenumbers range went from 4000 to 650 cm^{-1}.

Gas chromatography - mass spectroscopy was achieved on a Thermo Scientific GC Trace 1300, equipped with a 30 x 0.25 mm TG5-MS column (5% phenyl methyl siloxane). This was coupled with a DSQ II single quadripole mass spectrometer detector with an electron ionization source of 70 eV. Mass spectra were recorded between 30 and 500 Da (equivalent *m/z*). Samples of 1 µl were injected and eluted with helium at a flow of 1.2 $ml.min^{-1}$ at a temperature equal to 300 °C. The predicted *m/z* values were determined using ACD/MS Fragmenter.

Isothermal Titration Calorimetry (ITC) measurements were performed with a TAM III multichannel calorimetric device with nanocalorimeters and a Micro Reaction System (TA Waters). ITC experiments were carried out in cells (hastelloy) with 800 µL of polymer solution, at 298 K and consist of 25 injections of 10 seconds with 10 µL of cation solution. The system is equipped with a gold paddle stirrer used at 45 rpm. In order to allow the system to stabilize between injections, the latter are spaced 45 min

apart. The dilution effect is evaluated under similar conditions (without polymer), and subtracted using NanoAnalyze software.

2.3. Synthesis of α-benzyl carboxylate-ε-caprolactone (BzCL)

Lithium diisopropylamide (25 mL, 184.37 mmol) was put into a two-neck round-bottom flask with dry THF (100 mL) at -78 °C. ε-Caprolactone (15 g, 131.69 mmol) dissolved in dry THF (300 mL) was added and the mixture was stirred at -78 °C during 1 hour. Then, benzyl chloroformate (22.46 g, 131.69 mmol) was added slowly under vigorous stirring and the solution was allowed to rise 0 °C for 3 hours. Reaction was quenched with a saturated solution of ammonium chloride (100 mL) and THF was evaporated under reduced pressure. Ethyl acetate (200 mL) was added to the crude material, and the resulting organic phase was washed with a saturated solution of ammonium chloride until a neutral pH was obtained. Then, two washes were achieved with distilled water (2x50 mL) and the organic phase was dried over anhydrous magnesium sulfate. The solvent was removed under reduced pressure leading to a yellow oil which was purified using a column chromatography on silica gel, with a diethyl ether/ethyl acetate mixture (70:30, v/v) as eluent. Finally, α-benzyl carboxylate-ε-caprolactone was obtained as a yellowish oil (yield: 45 %).

^{1}H NMR (400 MHz, $CDCl_3$, δ (ppm)): 7.36 (m, 5H, CH aromatic, Ha), 5.21 (s, 2H, CH_2-Benzyl, Hb), 4.25-4.16 (m, 2H, CH_2-O, Hc), 3.75 (dd, 1H, CH, Hd), 2.11-1.59 (m, 6H, CH_2-CH_2-CH_2, He).

^{13}C NMR (400 MHz, $CDCl_3$, δ (ppm)) (Fig. S1): 171.9-168.87 (C=O, C4, C6), 135.34 (HC=C(CH)-CH_2, C2), 128.44 (C aromatic, C1), 69.43 (C-CH_2-O, C3), 67.37 (CH_2-CH_2-O, C7), 50.87 (CH, C5), 28.65, 26.94, 25.83 (CH_2-CH_2-CH_2, C8).

IR (σ (cm^{-1})): 2938 (CH); 1721 and 1700 (C=O).

Mass spectrum (*m/z* ($g.mol^{-1}$)): 247.09 $[M+H]^+$.

^{13}C NMR, COSY NMR, InfraRed and mass spectroscopy spectra are reported in the Supplementary Data (Fig. S1, Fig. S2, Fig. S3, and Fig. S4, respectively).

*2.4. Synthesis of poly(εCL-*st*-αBzεCL)-b-PEG-b-poly(εCL-*st*-αBzεCL)*

Copolymers of poly(εCL-*st*-αBzεCL)-*b*-PEG-*b*-poly(εCL-*st*-αBzεCL) with different εCL/BzCL ratios were synthesized by ring-opening polymerization of α-benzyl carboxylate-ε-caprolactone and ε-caprolactone, using poly(ethylene glycol) (PEG, M_n = 2000 g.mol^{-1}) as macro-initiator and tin(II) octanoate as catalyst. The typical protocol used for the synthesis of these copolymers is as follow (shown here for a εCL/BzCL ratio equal to 75/25, $PB_{25\%}$): α-benzyl carboxylate-ε-caprolactone (0.210 g, 0.85 mmol), ε-caprolactone (0.29 g, 2.54 mmol), PEG (0.5 g, 0.25 mmol) and tin octanoate (41 mg, 0.1 mmol) were added into a Schlenk under dry nitrogen atmosphere with dry toluene (5 mL). The reactional mixture was kept at 100 °C for 24 hours. Then, it was cooled to room temperature and concentrated under reduced pressure. The crude material was dissolved in a minimum of dichloromethane and precipitated in cold diethyl ether. Finally, the obtained polymer was dried under vacuum and recovered as a yellowish-white powder (yield: 57 %).

^{1}H NMR (400 MHz, $CDCl_3$, δ (ppm)): 7.27 (m, 5H, aromatic CH, Hl), 5.10 (s, 2H, CH_2-Ph (PαBzεCL), Hk), 3.99 (m, 4H, O-CH_2-CH_2- (PαBzεCL + PCL), Ha, Hf), 3.57 (s, 4H, CH_2-CH_2 (PEG) Hm), 3.31 (m, 1H, CH(C(O)OBz) (PαBzεCL), Hj), 2.28 (m, 2H, C(O)-CH_2-CH_2 (PCL), He), 1.85 (m, 2H, CH(C(O)OBz)-CH_2-CH_2 (PαBzεCL), Hi), 1.57 (m, 6H, OCH_2-CH_2-CH_2-CH_2 (PCL), CH_2-CH_2-CH_2-O (PαBzεCL), Hb, Hd, Hg), 1.31 (OCH_2-CH_2-CH_2-CH_2 (PCL), CH(C(O)OBz)-CH_2-CH_2 (PαBzεCL), Hc, Hh).

^{13}C NMR (400 MHz, $CDCl_3$, δ (ppm)) (Fig. S7): 173.55 (CH_2-C(O) (PCL), CH-C(O) (PαBzεCL), C6, C12), 169.11 (CH-C(O), C13), 137.83 (C_{quat}, aromatic, C15), 128.19 (CH aromatic, C16), 70.51 (CH_2-CH_2 (PEG), C17), 66.99 (O-CH_2-C, C14), 64.12 (CH_2-CH_2-O (PCL), C1), 63.42 (CH_2-CH_2-O (PαBzεCL), C7), 51.79 (CH (PαBzεCL), C11), 34.08 (C(O)-CH_2 (PCL), C5), 32.28 (CH-CH_2 (PαBzεCL), C10), 28.30 (O-CH_2-CH_2 (PαBzεCL + PCL), C2, C8), 25.49 (O-CH_2-CH_2-CH_2 (PαBzεCL + PCL), C3, C9), 24.54 (C(O)-CH_2-CH_2 (PCL), C4) (see Fig. S7 for labeling).

$SEC_{(THF)}$: M_n = 10000 g.mol^{-1}, $Đ$ = 1.55

^{1}H NMR spectra for $PB_{10\%}$, and $PB_{50\%}$ are reported in the Supplementary Data (Fig. S5, Fig. S6, respectively). ^{13}C NMR spectrum for $PB_{25\%}$ is reported in the Supplementary Data (Fig. S7). Size exclusion chromatograms are reported in the Supplementary Data for $PB_{10\%}$, and $PB_{50\%}$ (Fig. S8 and Fig. S9, respectively).

*2.5. Synthesis of poly(εCL-*st*-αCOOHεCL)-b-PEG-b-poly(εCL-*st*-αCOOHεCL)*

Benzyl groups of poly(εCL-*st*-αBzεCL)-*b*-PEG-*b*-poly(εCL-*st*-αBzεCL) copolymers were removed by catalytic hydrogenation, using dihydrogen and palladium on activated carbon as catalyst, in order to obtain carboxylic acid functions. The protocol used is as follows: the poly(εCL-*st*-αBzεCL)-*b*-PEG-*b*-poly(εCL-*st*-αBzεCL) copolymer ($PA_{25\%}$, 1 g) was dissolved in ethyl acetate (15 mL) in a flask and palladium on activated carbon (200 mg) was added. Then, vacuum/dihydrogen cycles were carried out and the flask was left under hydrogen with vigorous stirring for 12 hours at room temperature. The reaction mixture was filtered off on celite to remove the catalyst. Ethyl acetate was evaporated under reduced pressure and resulting acidic acid-based copolymer was dried under vacuum, leading to a white powder (yield: 98 %).

^{1}H NMR (400 MHz, $CDCl_3$, δ (ppm)): 4.03 (m, 4H, O-C$\underline{H}_2$-CH_2- (PαCOOHεCL + PCL), Ha, Hf), 3.61 (s, 4H, C$\underline{H}_2$-C$\underline{H}_2$ (PEG), Hm), 3.29 (m, 1H, C$\underline{H}$COOH (PαCOOHεCL), Hj), 2.28 (m, 2H, C(O)-C$\underline{H}_2$-CH_2 (PCL), He), 1.89 (m, 2H, CH-C$\underline{H}_2$-CH_2 (PαCOOHεCL), Hi), 1.61 (m, 6H, OCH_2-C$\underline{H}_2$-CH_2-C$\underline{H}_2$-C(O) (PCL), CH_2-C$\underline{H}_2$-CH_2-O (PαCOOHεCL), Hb, Hd, Hg), 1.36 (C(O)-CH_2-CH_2-C$\underline{H}_2$-CH_2 (PCL), CH(COOH)-CH_2-C$\underline{H}_2$ (PαCOOHεCL), Hc, Hh).

^{13}C NMR (400 MHz, $CDCl_3$, δ (ppm)) (Fig. S7): 173.54 (CH_2-C(O) (PCL), CH-C(O) (PαCOOHεCL), C6, C12), 169.10 (CH-C(O), C13), 70.54 (C$\underline{H}_2$-C$\underline{H}_2$ (PEG), C17), 64.13 (CH_2-C$\underline{H}_2$-O (PCL), C1), 63.43 (CH_2-C$\underline{H}_2$-O (PαCOOHεCL), C7), 51.80 (C$\underline{H}$ (PαCOOHεCL), C11), 34.10 (C(O)-C$\underline{H}_2$ (PCL), C5), 32.29 (CH-C$\underline{H}_2$ (PαCOOHεCL), C10), 28.32 (O-CH_2-C$\underline{H}_2$ (PαCOOHεCL + PCL), C2, C8), 25.50 (O-CH_2-CH_2-C$\underline{H}_2$ (PαCOOHεCL + PCL), C3, C9), 24.55 (C(O)-CH_2-C$\underline{H}_2$ (PCL), C4) (see Fig. S7 for labeling).

$SEC_{(THF)}$: M_n = 9000 g.mol^{-1}, $Đ$ = 1.77

^{1}H NMR spectra for $PA_{10\%}$, and $PA_{50\%}$ are reported in the Supplementary Data (Fig. S5, Fig. S6, respectively). ^{13}C NMR spectrum for $PA_{25\%}$ is reported in the Supplementary Data (Fig. S7). Size exclusion chromatograms are reported in the Supplementary Data for $PA_{10\%}$, and $PA_{50\%}$ (Fig. S8 and Fig. S9, respectively).

2.6. Solutions for Isothermal Titration Calorimetry

Preparation of polymeric aqueous solutions

Aqueous solutions of polymers were prepared by dissolving each polymer in a precise amount of Milli-Q water and the pH was adjusted to reach 5.5 with acidic solution (0.5 mol.L^{-1} HNO_3) or basic solution (0.5 mol.L^{-1} NaOH). Polymer solutions (for $PA_{10\%}$, $PA_{25\%}$, $PA_{50\%}$) were prepared at concentrations equal to 10, 3 and 3 g.L^{-1}, respectively.

Preparation of cation aqueous solutions

Aqueous solutions of cations (Nd(III) and Ce(III)) were prepared by dissolving neodymium (III) nitrate hexahydrate or cerium (III) nitrate hexahydrate in Milli-Q water and the pH was adjusted at pH 5.5, as done for the solutions of polymers. The concentration was 3 mM for all polymers ($PA_{10\%}$, $PA_{25\%}$, $PA_{50\%}$) and it was the same for Nd(III) and Ce(III) solutions.

3. Results and discussion

3.1. Monomer and polymers synthesis

First work consisted in the synthesis of appropriate functional copolymers, namely the poly(εCL-*st*-αCOOHεCL)-*b*-PEG-*b*-poly(εCL-*st*-αCOOHεCL) copolymers. First, the synthesis of a functional ε-caprolactone monomer bearing protecting group on carboxylic acid function was achieved (Scheme 1). α-Benzyl carboxylate-ε-caprolactone (BzCL) monomer was prepared as benzyl groups can be easily removed by hydrogenation to afford complexing carboxylic acid groups.

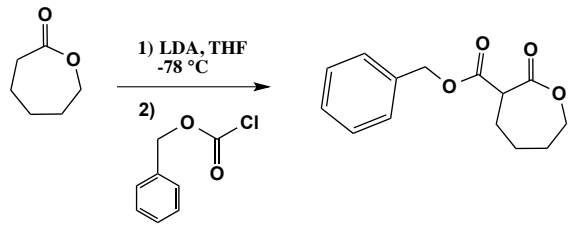

Scheme 1. Reactional pathway for the synthesis of functional α-benzyl carboxylate-ε-caprolactone (BzCL) monomer.

Functionalization of ε-caprolactone (εCL) was based on the anionic activation in the presence of lithium diisopropylamide (LDA), followed by electrophilic substitution *via* benzyl chloroformate. The synthesis of functional εCL was carried out according to a protocol described by Mahmud *et al.* [55], which was slightly modified (notably with the use of commercial LDA and another procedure for the purification step). The BzCL monomer was purified by column chromatography on silica gel, using a diethyl ether/ethyl acetate eluent (70/30, v/v). Reaction yield was about 45% because of side reactions occurring during the synthesis, in particular the synthesis of oligomers by-products during the anion activation step. After purification by column chromatography on silica gel, with a diethyl ether/ethyl acetate mixture (70/30, v/v) as eluent, characterization by ^{1}H NMR (Fig. 1) proved that the reaction was successful, notably with signals at 5.4 and 7.2-7.4 ppm, corresponding to the methylene and the aromatic protons of the benzyl group, respectively. The structure was also confirmed by ^{13}C NMR, COSY NMR, IR, and mass spectrum (Supplementary Data, Fig. S1, Fig. S2, Fig. S3, and Fig. S4, respectively).

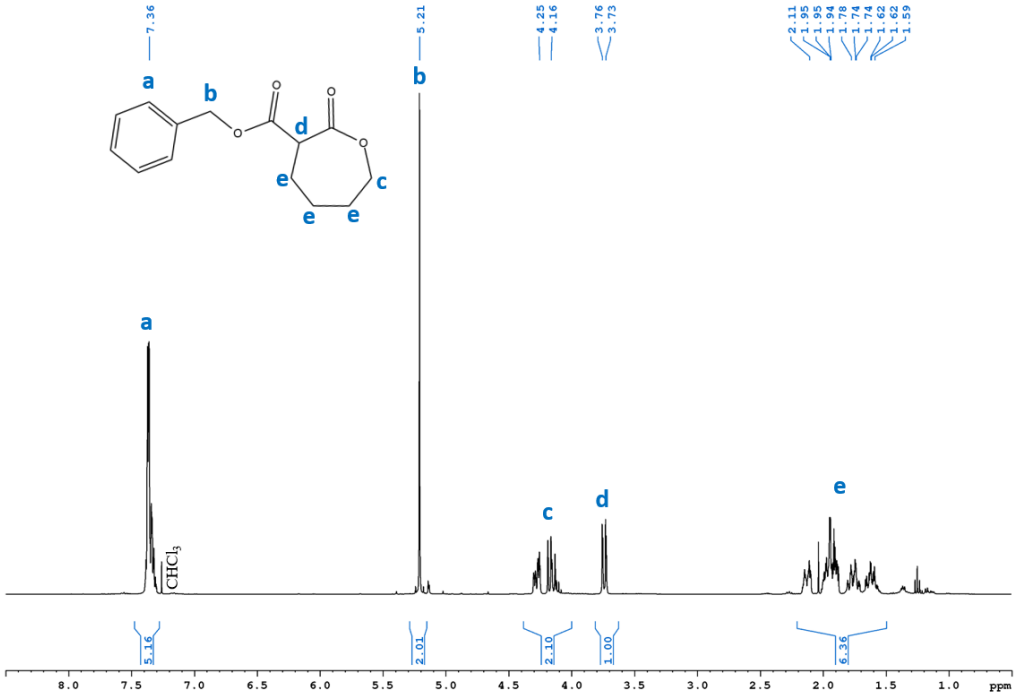

Fig. 1. ^{1}H NMR spectrum of α-benzyl carboxylate-ε-caprolactone (BzCL) in $CDCl_3$.

Then, BzCL was copolymerized with ε-caprolactone, in the presence of polyethylene glycol (PEG, M_n = 2000 g.mol^{-1}) as macro-initiator, by ring-opening polymerization (ROP) in toluene solution at 100 °C (Scheme 2). Tin(III) octanoate was chosen as the catalyst because it is approved by the FDA [56], which will be useful if resulting copolymers will be employed for biological applications. A series of poly(εCL-*st*-αCOOHεCL)-*b*-PEG-*b*-poly(εCL-*st*-αCOOHεCL) copolymers with different εCL/BzCL ratios was synthesized (Table 1), targeting in all cases total molar masses equal to 4000 g.mol^{-1}, in order to only study the effect of the increase of the εCL/BzCL ratio on the complexing properties, after deprotection of the benzyl groups to afford carboxylic acid functions. Three different εCL/BzCL theoretical ratios were employed, equal to 90/10, 75/25, and 50/50, leading to corresponding copolymers, namely $PB_{10\%}$, $PB_{25\%}$, and $PB_{50\%}$, respectively.

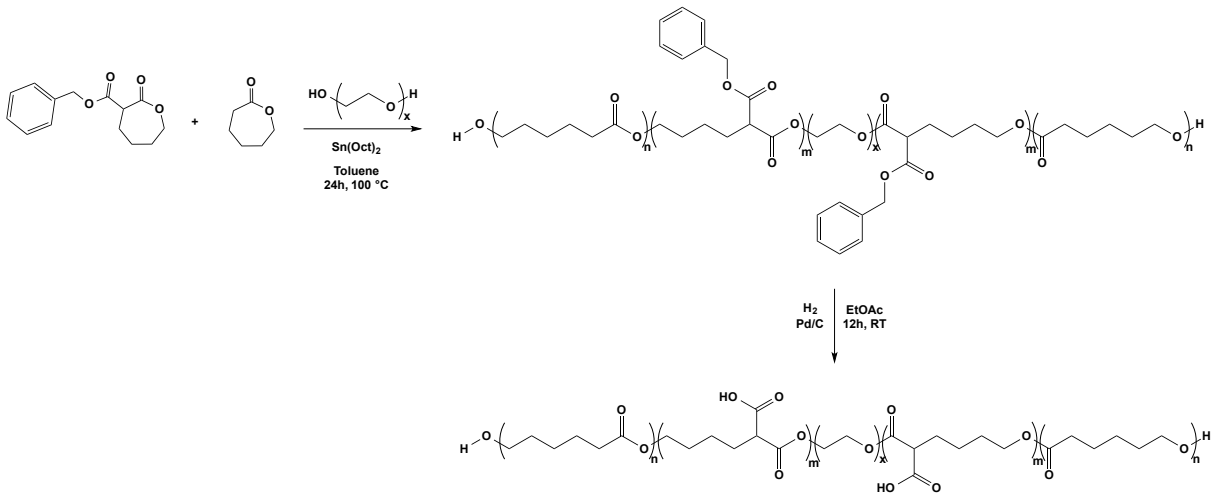

Scheme 2. Reactional pathway for the synthesis of functional poly(εCL-*st*-αCOOHεCL)-*b*-PEG-*b*-poly(εCL-*st*-αCOOHεCL) copolymers.

Table 1.

General characteristics of synthesized copolymers (with X = Bz or COOH).

Copolymer	Theoretical εCL/αXεCL ratio	Experimental εCL/αXεCL ratio [b]	$M_{n,\,theo}$ [a] (g.mol^{-1})	$M_{n,\,exp}$ [b] (g.mol^{-1})	$M_{n,\,exp}$ [c] (g.mol^{-1})	*Đ*	Yield (%)
$PB_{10\%}$ [d]	90/10	92/08	4000	4800	5400	1.52	60
$PA_{10\%}$ [e]	90/10	92/08	3800	4500	5000	1.59	98
$PB_{25\%}$	75/25	75/25	4000	3600	5800	1.55	57
$PA_{25\%}$	75/25	75/25	3700	3400	5200	1.77	98
$PB_{50\%}$	50/50	60/40	4000	3100	7000	1.31	55
$PA_{50\%}$	50/50	61/39	3500	2700	6500	1.35	96

[a] determined using M_n = [M]/[A] x conversion; [b] determined by ^{1}H NMR; [c] determined by size exclusion chromatography with THF as eluent and PMMA as standards; [d] PB: poly(εCL-*st*-αBzεCL)-*b*-PEG-*b*-poly(εCL-*st*-αBzεCL); [e] PA: poly(εCL-*st*-αCOOHεCL)-*b*-PEG-*b*-poly(εCL-*st*-αCOOHεCL).

After evaporation of the toluene, the crude material was dissolved in a minimum of dichloromethane and precipitated in cold diethyl ether. ^{1}H NMR spectra of resulting copolymers (Fig. 2 for $PB_{25\%}$ and Fig. S5, Fig. S6 for $PB_{10\%}$, $PB_{50\%}$, respectively) proved that the copolymerization was successful. In particular, signals at 3.31 and 5.1 ppm corresponded to the CH in the α-position of the benzyl group (proton j) and to the methylene of the benzyl group (proton k), respectively, whereas signal at 2.28

ppm (proton e) was attributed to the methylene in the α-position of the ester function in the ε-caprolactone unit. Furthermore, experimental εCL/BzCL could be calculated by comparing the integration of the signal at 2.28 ppm (-C<u>H</u>$_2$-C(O)O- in the εCL unit, proton e) with the integration of either the same signal at 3.31 ppm ((-C<u>H</u>(Bz)-C(O)O- in the BzCL unit, proton j) or signal at 1.85 ppm (-CH-C<u>H</u>$_2$-CH- in the BzCL unit, proton i) for comparison and confirmation. Whatever the prepared copolymer, experimental ratios were close from theoretical ones (Table 1). In the case of the $PB_{50\%}$, ratio was slightly lower (around 40%). Overall, we prepared three different copolymers varying experimental εCL/BzCL ratio from 8 to 39 %. It is important to note that copolymerization with εCL/BzCL ratios equal to 25/75 and 0/100 led to low monomer conversion. Indeed, the reactivity of BzCL was too low due to steric hindrance of the benzyl ring.

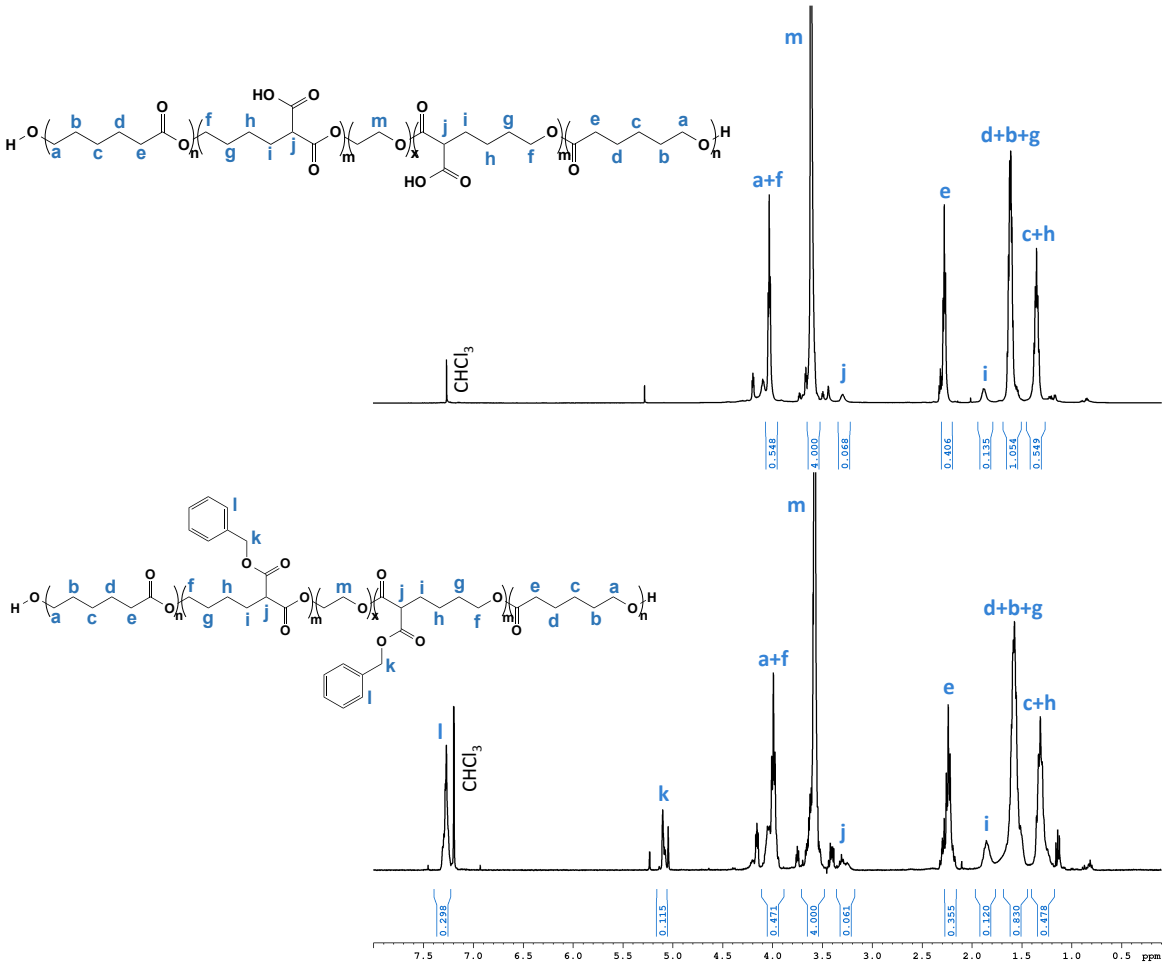

Fig. 2. ^{1}H NMR spectra of $PB_{25\%}$ (bottom) and $PA_{25\%}$ (top) (in $CDCl_3$).

^{1}H NMR also allowed the calculation of the molecular weight (M_n) of the synthesized copolymers by comparison of signals of εCL and BzCL (protons e and j, respectively) with the one corresponding to the ethylene glycol unit at 3.57 ppm (proton m). Experimental molecular weights were close from theoretical ones whatever the εCL/BzCL ratio used. Copolymers were also characterized by size exclusion chromatography (SEC) in THF (Fig. 3 for $PB_{25\%}$, Fig. S8 and Fig. S9 for $PB_{10\%}$ and $PB_{50\%}$, respectively) calibrated with poly(methyl methacrylate) standards, which showed a monomodal signal, thus confirming the presence of a single polymer population. Concerning $PB_{50\%}$, bimodal SEC trace (Fig. S9) was obtained, demonstrating a poor control of the polymerization. This was due to the high proportion of the bulky α-benzyl carboxylate-ε-caprolactone, which showed low reactivity. Dispersities (*Đ*) varied from 1.31 to 1.55, which is commonly obtained for polymers prepared by ring opening copolymerization [57].

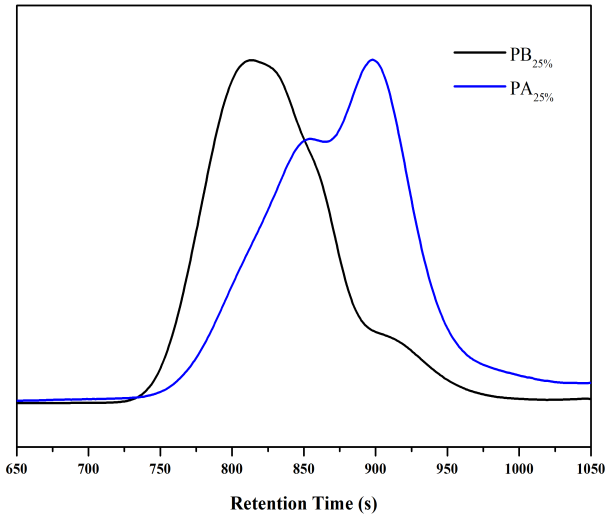

Fig. 3. SEC spectrum of $PB_{25\%}$ in black and $PA_{25\%}$ in blue (eluent: THF, standards: PMMA).

Last step of the synthesis dealt with the deprotection of the benzyl groups to afford carboxylic acid functions, able to efficiently complex actinides. For such purpose, hydrogenation of copolymers ($PB_{10\%}$, $PB_{25\%}$, $PB_{50\%}$) was carried out in ethyl acetate in the presence of palladium on activated carbon as catalyst, under pressure, during 12 hours. Poly(εCL-*st*-αCOOHεCL)-*b*-PEG-*b*-poly(εCL-*st*-αCOOHεCL) ($PA_{10\%}$,

$PA_{25\%}$, $PA_{50\%}$) copolymers were obtained in quantitative yields as white powders after filtration on celite and evaporation of ethyl acetate. Acidic acid-based copolymers were characterized by ^{1}H NMR (Fig. 2 for $PA_{25\%}$, Fig. S5 and Fig. S6 for $PA_{10\%}$ and $PA_{50\%}$, respectively). We noticed the logical disappearance of the peaks corresponding to the benzyl groups, at 7.27 (protons l) and 5.10 ppm (protons k) for the aromatic protons and the methylene, respectively. The other peaks characteristic of the copolymers backbones showed the same chemical shift, proving that no significant degradation occurred during the hydrogenation. Once again, it was possible to calculate both the εCL/BzCL ratio and the molecular weight by ^{1}H NMR (Table 1). Concerning the ratio, comparison of the integrations of the signal at 2.28 (-C$\underline{H}_2$-C(O)O- in the εCL unit, proton e) and either 3.29 ppm ((-C$\underline{H}$(COOH))-C(O)O- in the COOHCL unit, proton j) or 1.89 ppm (-CH-C$\underline{H}_2$-CH- in the COOHCL unit, proton i), for comparison and confirmation, led to the same values than before the hydrogenation step. Additionally, comparison of integrations of protons at 2.28 and 3.29 ppm (-C(O)-C$\underline{H}_2$-CH_2 in the PCL unit (protons e) and -C$\underline{H}$(C(O)OH) (proton j), respectively) with the one at 3.61 ppm attributed to the methylene groups of the PEG moiety, allowed to evaluate the molecular weight. As expected, PA copolymers showed lower molecular weights than the benzyl-based PB due to the loss of the benzyl group during the deprotection step. Size exclusion chromatography (Fig. 3) gave same trend, with longer retention times, confirming the logical decrease in the molecular weights for PA in comparison with PB copolymers. Dispersities slightly increased, going from 1.35 to 1.77. This was due to the obtaining of bimodal traces as the polar character of the carboxylic acid functions made the copolymers more retained on the SEC columns. More generally, the higher the functionalization rate in polar group (benzyl or acidic) was, the more polymers were retained on the chromatographic columns.

To conclude, we managed to prepare three different poly(εCL-st-αCOOHεCL)-*b*-PEG-*b*-poly(εCL-st-αCOOHεCL) copolymers with comparable molecular weight (around 4000 g.mol^{-1}) and experimental acidic acid functionalization rate equal to 8, 25 and 39 %, namely $PA_{10\%}$, $PA_{25\%}$, and $PA_{50\%}$. These copolymers were of great interest as they were water soluble and based on poly(ethylene glycol) and poly(ε-caprolactone), which are both biocompatible. As a result, these materials could be used for actinide body decontamination. It is important to mention that, to date, only

very few synthetic polymeric systems were considered for such application. In order to evaluate sorption properties, studies of complexation of these three copolymers possessing different carboxylic acid function rates were carried out with two different cations (neodymium (III) and cerium (III), surrogates of actinides). Sorption rates were determined and influence of the functionalization rate on the complexing properties (capacities and binding affinity) of the prepared copolymers was also studied.

3.2. Sorption study

Cation complexation studies were carried out using Isothermal Titration Calorimetry (ITC) with the three acidic acid-based copolymers ($PA_{10\%}$, $PA_{25\%}$, and $PA_{50\%}$). The ITC results were used to select the most promising polymers, as well as to understand the driving forces of the interactions [58], in particular to evaluate the efficiency as a function of the level of carboxylic acid functions present within the copolymers. Sorption efficiency was evaluated with neodymium (Nd(III)) and cerium (Ce(III)) because these elements belonging to the lanthanides serve as surrogate of actinides, the latter being riskier to use. Preliminary speciation diagrams were established to confirm the ionic species present in solution in the required experimental conditions. Insoluble lanthanide hydroxides are known to form above pH 6. All tests were done at pH 5.5 to be suitable taking into account cations speciation. It is worth noting that this pH also corresponded to the skin, which indicates that obtained results are of interest for potential treatment of external decontamination. The thermodynamic parameters presented here were condition-dependent. Complexation tests with thorium (Th) were also carried out, but at pH 5.5 this element was not available strictly in ionic form and therefore could not be complexed by polymers.

Aqueous solutions of each copolymers and cations were prepared, and ITC measurements were carried out at 25 °C. The typical thermograms obtained are shown in Fig. 4 (and ITC thermograph (top) and titration curve (bottom) in Supplementary Data, with Fig. S10 for $PA_{25\%}$ and Ce(III), Fig. S11 for for $PA_{10\%}$ and Nd(III), Fig. S12 for $PA_{10\%}$ and Ce(III), Fig. S13 for for $PA_{50\%}$ and Nd(III), and Fig. S14 for for $PA_{50\%}$ and Ce(III)). The peaks corresponding to the complexation of Nd (in

black) were initially endothermic, with a minimum heat rate of -1.3 µW. As the injections progressed, the heat rate approached 0, until an endothermic/exothermic transition, and exothermic stabilization around 0.35-0.4 µW, after about 18-20 injections. By comparison, the peaks in gray represent the dilution, that is, the injection of the cation solution into water only (without polymer). Thus, the only effects were the effects of dilution of the cationic solution and the peaks were all exothermic with a constant heat rate around 0.4 µW. This demonstrated that for $PA_{25\%}$ solution from 18-20 injections, only the dilution effects were detected. This absence of significant signal suggested that interaction and complexation no longer took place. This meant that all the complexing sites of the carboxylic acids of the polymer were occupied by cations and therefore the polymer was saturated, no longer being able to chelate other Nd ions. In other words, the maximum complexing capacity of the polymer has been reached.

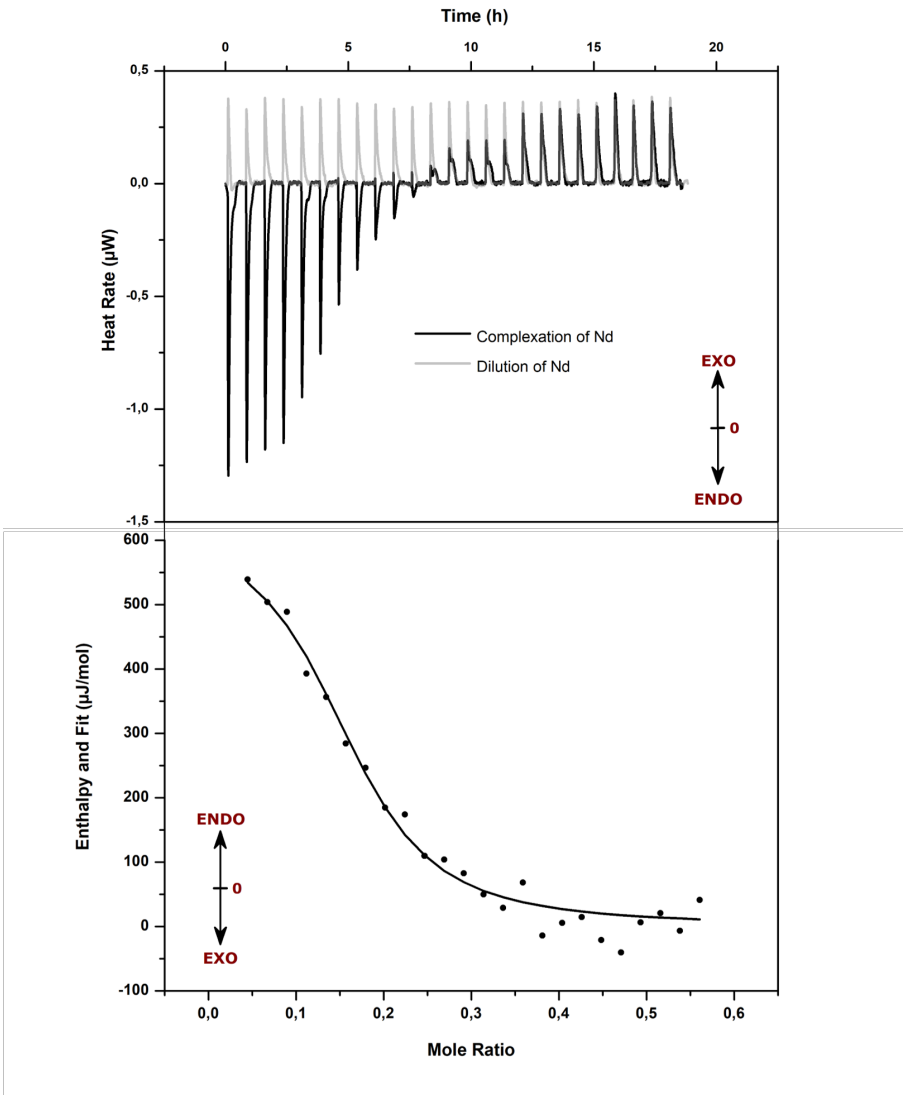

Fig. 4. Isothermal Titration Calorimetry (ITC) thermograph (top) and titration curve (bottom) corresponding to $PA_{25\%}$ in the presence of Nd(III).

Subsequently, by integrating the area under the curve of each peak of the thermogram, the titration curve was obtained (Fig. 4, bottom) and represented the enthalpy of reaction as a function of the molar ratio (mole cation/mole polymer). Thus, after appropriate curve fitting using one set of site-binding model, this curve provided the thermodynamic parameters of the system, such as stoichiometry (n), bond strength (K_a or K_d), and enthalpy (ΔH). Gibbs free energy (ΔG) and changes in entropy ($T\Delta S$) could then be calculated. The thermodynamic parameters resulting from the complexation of the three polymers with Nd(III) and Ce(III) are summarized on Fig. 5. At the top left is the graph representing the stoichiometry expressed as the number of carboxylic acid functions necessary to complex one ion (Nd(III) or Ce(III)),

for the various copolymers. It appeared that whatever the complexed cation, $PA_{10\%}$ was the polymer that required the largest number of complexing groups to chelate a cation. Conversely, $PA_{25\%}$ was the polymer that complexed the most ions with the fewest carboxylic acid functions. However, by further increasing the quantity of complexing functions within the polymer ($PA_{50\%}$), the quantity of these functions necessary for the complexation of one cation increased again, meaning that the optimal polymer for chelating a maximum of ions was that containing 25% carboxylic acid groups ($PA_{25\%}$). Fig. 5 also exhibited the binding constants of the three copolymers with Nd(III) or Ce(III). The constants were in the range of 3-8 10^3 M^{-1}. Generally speaking, the range of the binding constant for sorption (complexation, exchange, adsorption) are in the range of 10^{+8} M^{-1} or even higher for strong interaction such as for multivalent carboxylate ligands to Ca(II) [59] or metal ions binding to the peptides [60]. In the case of low-cost sorbents (biopolymer, clays, zeolites, etc.) the affinity is lower, with relative weak binding sites [61]. Our results were in the range of average value for the complexation. For Nd(III), with log K between 3.58 and 3.92, our results were similar to the one obtained for acetates [62], lactate [63] or gluconate [64]. Our data gave log K in the range 3.46 et 3.82 for Ce(III). This was lower that other complexation systems, such as cyclic diaza diacetates (Log K 12.2, à 10.9) [65], but only slightly smaller than binding with Bovine Liver Catalase (BLC) [66] in the particular case of the induced conformational changes of BLC in presence of Ce(III). For Nd(III), the binding constant was the greatest for $PA_{25\%}$ meaning that not only this polymer was able to complex more cations than the others, but also the bonds were stronger, promising better extraction. This has been observed by Sánchez-Fernández *et al.* [67] with systems based on poly(2-oxazoline)s functionalized with controllable amounts of alendronate, hydroxyl, and carboxylic acid side groups. In this study, having multiple alendronates along the polymer backbone obviously led to improved binding. Regarding Ce(III), the binding constants were lower for the three copolymers, and $PA_{10\%}$ was the one with the highest (6500 M^{-1}).

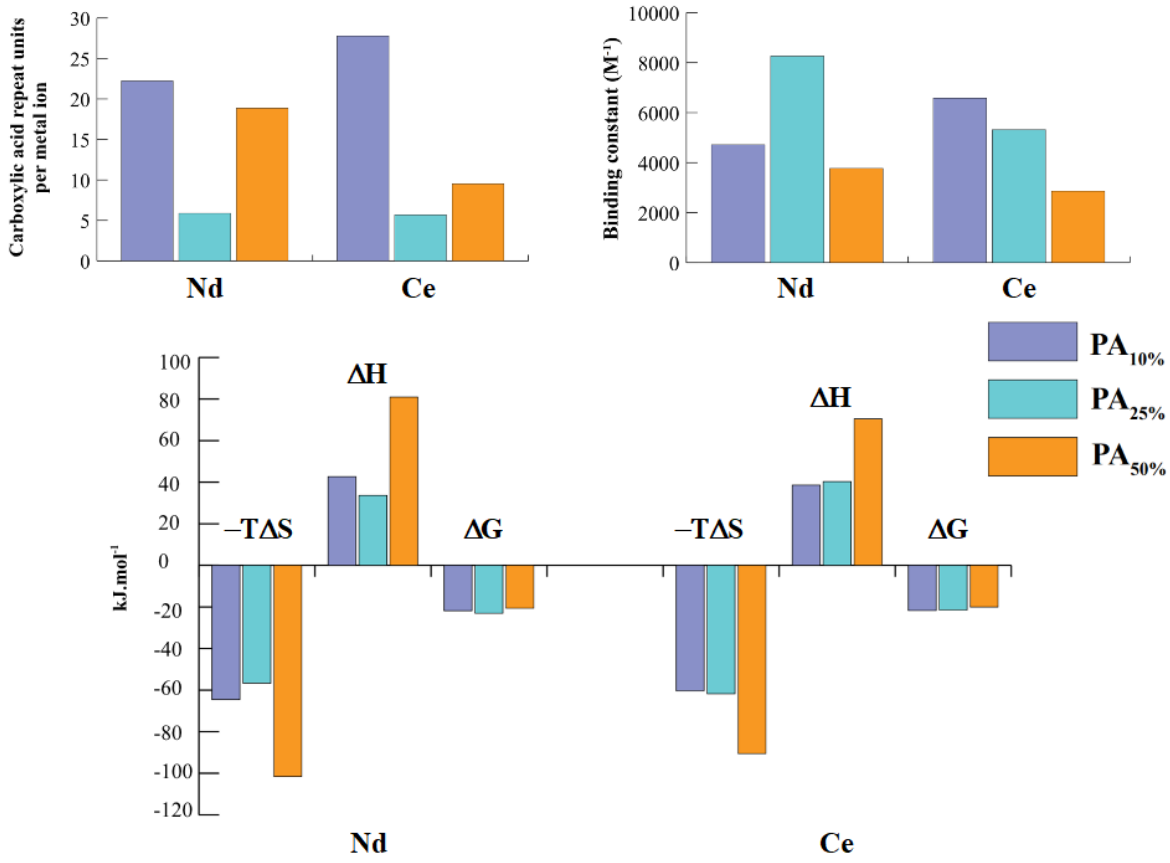

Fig. 5. On the top left corner, stoichiometry of metal ions binding for the three copolymers functionalized; on the top right corner, binding constants of the three copolymers with the metal ions; on the bottom, thermodynamic constants of Nd(III) and Ce(III) binding to the three copolymers.

Despite everything, the constant of $PA_{25\%}$ was quite close (5500 M^{-1}). In all cases, the constants of $PA_{50\%}$ were the lowest, showing that even when many carboxylic acid functions were present in the polymer chain and were linked to the same cation, their binding energy was lower, with poor retention, running the risk of "releasing" the ion before being extracted from contaminated medium. Finally, the last graph (Fig. 5, bottom) gave the thermodynamic constants (the change in entropy ΔS, enthalpy ΔH, and free energy ΔG) of the copolymers according to the complexed cation. Thus, in all cases, each cation-polymer interaction was endothermic. Whatever the ion and the polymer, each system was directed by entropy, the variations of which were slightly greater than those of enthalpy. This entropically-driven thermodynamic profile with sometimes high positive ΔS occurred because of a release of complexed water molecules, as well as counterions and the reduction of long-range solvent ordering

during binding [68]. Also, the positive values of ΔS for both metal ions indicated that the degree of randomness at the interface during the complexation process increased or the sorption involved the liberation of more ions when discrete metal ions were bound to the sorbent. This increase in the entropy of the system was also observed by Teodoro *et al.* [69] on carboxylated cellulose derivative, where the entropic contribution was attributed to the water molecules that were released from desolvation of the metal ions and adsorption sites (carboxylic acid groups) adsorbent surface.

The obtained ITC stoichiometry data suggested that polymers functionalized served as an effective and efficient multidentate ligand when binding to rare earth elements (REEs). The maximum sorption capacities (q_{max}) of the three synthesized copolymers were calculated from the obtained stoichiometry and then compared with those found in the literature for different systems used for Nd(III) or Ce(III) removal by complexation, adsorption or exchange. The sorption capacity represented the quantity of cations absorbed (in mg) per gram of polymer. Thus, Table 2 compares the Nd(III) sorption capacities of different materials, at different pH.

Table 2.

Comparison of sorption efficiencies of different sorbents for Nd(III) ions.

Sorbent	**pH**	**Sorption capacity ($mg.g^{-1}$)**	**Reference**
Transcarpathian clinoptilolite (Zeolite)	6.5	1.81	[70]
Carbonized parachlorella 250 °C	7	5.53	[71]
Impregnated SiO_2/UF composite	3	4.959	[72]
Cyphos@silica	4	13.4	[73]
Silica gel modified with diglycol amic acid	1	16.15	[74]
Chitosan/Iron(III) hydroxide	4	13.8	[75]
Microorganisms	1.5	10-12	[76]
Magnetic nano-hydroxyapatite	5.5	323	[77]
$PA_{10\%}$	5.5	2.62	This work
$PA_{25\%}$	5.5	13.63	This work
$PA_{50\%}$	5.5	5.38	This work

It is important to note that complexing materials were not necessarily polymers and therefore their sorption mechanism could be totally different. This may explain the differences in q_{max}, such as for magnetic nano-hydroxyapatite, whose q_{max} (323 $mg.g^{-1}$) was extremely high. In this work, Gok *et al.* [77] obtained similar thermodynamic parameters as the one obtained in the present study. Otherwise, $PA_{25\%}$ had a q_{max} whose value was close to, or even greater than that of most of the materials used for the complexation of Nd(III). The $PA_{10\%}$ and $PA_{50\%}$ had a lower sorption capacity, but remained within the average of those found for many systems.

The same comparison was carried out for the complexation of Ce(III) (Table 3). In this case, most of the q_{max} described in the literature were higher than those obtained for the three studied copolymers. For instance, in the case of biosorption on *Platanus orientalis* leaf [78], their sorption capacities were higher than in the present study but the thermodynamics parameter (binding constant) were in favor of the PA copolymers. However, the only polymeric system described (polymer supported o-vanillinsemicarbazone) had a sorption capacity lower than $PA_{25\%}$ and $PA_{50\%}$, and almost equal to $PA_{10\%}$, once again demonstrating the effectiveness of these copolymers in the complexation of cations (in particular $PA_{25\%}$). In addition, as for the previous results, the $PA_{50\%}$ had a lower complexing capacity than the $PA_{25\%}$, while the number of complexing functions present within the copolymer was greater. This could be explained by the fact that the high number of acid functions (50%) and their vicinity, modifies both the strength of interaction and the accessibility. The proximity between chelating groups yields steric hindrance between sorption sites within the polymer. Once the first cations were sorbed, the accessibility seems to reach a maximum, and access for further cations was impeded. In addition, the polymer chains in solution might form interchain complexes [79] and therefore some of the complexing groups might be no longer similarly available for the chelation of cations, thus reducing its complexation efficiency. These results therefore showed that with $PA_{25\%}$, the optimum quantity of complexing functions within the copolymer had been reached, in order to guarantee the best complexing properties of the Nd(III) and Ce(III) ions.

Table 3.

Comparison of sorption efficiencies of different sorbents for Ce(III) ions.

Sorbent	**pH**	**Sorption capacity ($mg.g^{-1}$)**	**Reference**
TPDP ligand / mesoporous silica monoliths	3.5	192.31	[80]
MnOOH	5.5	45.5	[81]
MnO_2	5.5	22.2	[81]
Mn_3O_4	5.5	7.7	[81]
Fe_3O_4	3.8	160	[82] (*)
Spirulina biomass	5.5	18.1	[83]
Polymer supported o-vanillinsemicarbazone	6-9	2.48	[84]
Platanus orientalis leaf powder	4	32.05	[78]
$PA_{10\%}$	5.5	2.04	This work
$PA_{25\%}$	5.5	13.71	This work
$PA_{50\%}$	5.5	10.35	This work

(*) In the considered contribution, the considered cation was Ce(IV).

4. Conclusion

The objective of this work was to develop original and valuable copolymers bearing pendant carboxylic acid functions for the complexation of radioactive elements (actinides). Thus, three copolymers with different carboxylic acid group ratios were synthesized and evaluated, notably to determine the ideal quantity of chelating groups for the optimal complexation of the studied elements. Concerning the synthesis, the α-benzyl carboxylate-ε-caprolactone monomer was first synthesized. Then, copolymerization of the latter with ε-caprolactone as comonomer using poly(ethylene glycol) as macro-initiator was carried out in the presence of tin octanoate as catalyst. Three different εCL/BzCl were targeted: 10, 25, and 50%, and molecular weight was equal to 4000 $g.mol^{-1}$ for all copolymers. Obtained results showed that experimental ratios were close from theoretical ones and that all copolymers had similar molecular weight. Then, hydrogenation in the presence of palladium on activated carbon allowed removing the benzyl groups to afford copolymers bearing carboxylic acid functions, namely $PA_{10\%}$, $PA_{25\%}$, and $PA_{50\%}$. Complexation studies were carried out by Isothermal Titration Calorimetry with Neodynium (III) and Cerium (III), chosen as surrogates of actinides. The results showed that $PA_{25\%}$ was the most efficient polymer capable of complexing Nd(III) and Ce(III), with the highest stoichiometry and sorption capacity. Thus, it has been shown that by increasing the amount of carboxylic acid functions within the polymer, the complexation did not necessarily increase, as $PA_{50\%}$ had a lower sorption capacity than $PA_{25\%}$. Indeed, the folding of the polymer chains led to a decrease in the availability of complexing sites and therefore a decrease in sorption.

Studies of complexation with other elements should be carried out, in particular with actinides such as uranium and plutonium. In addition, biocompatibility and toxicity studies of the final polymers should be evaluated, in order to check that the presence of acid groups did not alter the biocompatibility of the materials. If conclusive results are obtained, poly(εCL-*st*-αCOOHεCL)-*b*-PEG-*b*-poly(εCL-*st*-αCOOHεCL) will be of great interest to be used for body decontamination, for which efficient solutions (even more involving synthetic functional polymers) are nowadays still rare.

Conflicts of interest

There are no conflicts to declare.

Declaration of Competing Interest

The authors declare that they have no known competing financial interests or personal relationships that could have appeared to influence the work reported in this paper.

Acknowledgements

The authors thank “Agence d’Innovation Défense” (AID) for funding this work (PhD grant (LF)), and ANR DECAP (ANR-18-ASTR-0001) (CAC)), and SynBio3 platform (IBMM, Montpellier) for the SEC analyses.

Appendix A. Supplementary Data

Supplementary data associated with this article can be found in the online version at doi:10.1016/j.reactfunctpolym.2016.xx.xxx.

References

[1] E.T. Cheng, Performance characteristics of actinide-burning fusion power plants, Fusion Sci. Technol. 47(4) (2005) 1219-1223.

[2] M. De Cesare, L.K. Fifield, C. Sabbarese, S.G. Tims, N. De Cesare, A. D'Onofrio, A. D'Arco, A.M. Esposito, A. Petraglia, V. Roca, F. Terrasi, Actinides AMS at CIRCE and U-236 and Pu measurements of structural and environmental samples from in and around a mothballed nuclear power plant, Nuclear Instruments & Methods in Physics Research Section B: Beam Interactions with Materials and Atoms 294 (2013) 152-159.

[3] W. Burkart, P.R. Danesi, J.H. Hendry, Properties, use and health effects of depleted uranium, in: T. Sugahara, H. Morishima, M. Sohrabi, Y. Sasaki, I. Hayata, S. Akiba (Eds.), High levels of natural radiation and radon areas: radiation dose and health effects, Elsevier Science Bv, Amsterdam, 2005, pp. 133-136.

[4] G. Choppin, Actinide chemistry: from weapons to remediation to stewardship, Radiochim. Acta 92(9-11) (2004) 519-523.

[5] S.S. Hare, I. Goddard, P. Ward, A. Naraghi, E.A. Dick, The radiological management of bomb blast injury, Clin. Radiol. 62(1) (2007) 1-9.

[6] T.D. Ippolito, Effects of variation of uranium enrichment on nuclear submarine reactor design, Massachusetts Institute of Technology, Massachusetts Institute of Technology, 1990, pp. 1-257.

[7] E.R. Birnbaum, M.E. Fassbender, M.G. Ferrier, K.D. John, T. Mastren, Actinides in medicine, Encyclopedia of Inorganic and Bioinorganic Chemistry (2018) 1-21.

[8] P.J. van Leeuwen, L. Emmett, B. Ho, W. Delprado, F. Ting, Q. Nguyen, P.D. Stricker, Prospective evaluation of 68Gallium-prostate-specific membrane antigen positron emission tomography/computed tomography for preoperative lymph node staging in prostate cancer, BJU International 119(2) (2017) 209-215.

[9] N.M. Griffiths, J.C. Wilk, M.C. Abram, D. Renault, Q. Chau, N. Helfer, C. Guichet, A. Van der Meeren, Internal contamination by actinides after wounding: a robust rodent model for assessment of local and distant actinide retention, Health Phys. 103(2) (2012) 187-194.

[10] F. Lahrouch, O. Sofronov, G. Creff, A. Rossberg, C. Hennig, C. Den Auwer, C. Di Giorgio, Polyethyleneimine methylphosphonate: towards the design of a new class of macromolecular actinide chelating agents in the case of human exposition, Dalton Trans. 46(40) (2017) 13869-13877.

[11] D. Pusset, H. Boulahdour, M. Fromm, J.L. Poncy, B. Kantelip, B. Griffond, M. Baud, P. Galle, Ultrastructural apoptotic lesions induced in bone marrow after neptunium-237 contamination, Anticancer Res. 23(6C) (2003) 4837-4842.

[12] G. Creff, S. Safi, J. Roques, H. Michel, A. Jeanson, P.L. Solari, C. Basset, E. Simoni, C. Vidaud, C. Den Auwer, Actinide(IV) Deposits on Bone: Potential Role of the Osteopontin Thorium Complex, Inorg. Chem. 55(1) (2016) 29-36.
[13] J.T. Edsall, Toxicity of plutonium and some other actinides, Bull. Atom. Scient. 32(7) (1976) 26-37.
[14] A. Durakovic, Medical effects of internal contamination with actinides: further controversy on depleted uranium and radioactive warfare, Environ. Health Prev. 21(3) (2016) 111-117.
[15] A. Tazrart, M.A. Bolzinger, S. Coudert, S. Lamart, B.W. Miller, J.F. Angulo, S. Briancon, N.M. Griffiths, Skin absorption of actinides: influence of solvents or chelates on skin penetration ex vivo, Int. J. Radiat. Biol. 93(6) (2017) 607-616.
[16] A. Tazrart, M.A. Bolzinger, S. Lamart, S. Coudert, J.F. Angulo, V. Jandard, S. Briancon, N.M. Griffiths, Actinide-contaminated skin: comparing decontamination efficacy of water, cleansing gels, and DTPA gels, Health Phys. 115(1) (2018) 12-20.
[17] E. Fattal, N. Tsapis, G. Phan, Novel drug delivery systems for actinides (uranium and plutonium) decontamination agents, Adv. Drug Deliv. Rev. 90 (2015) 40-54.
[18] K.L. Nash, P.G. Rickert, E. Lessman, M. Mendoza, J. Feil, J.C. Sullivan, New water-soluble phosphonate and polycarboxylate complexants for enhanced f-element separations, Abstr. Pap. Am. Chem. Soc. 207 (1994) 177.
[19] G.N. Stradling, Decorporation of actinides: a review of recent research, J. Alloy. Compd. 271 (1998) 72-77.
[20] A.J. Francis, C.J. Dodge, J.A. McDonald, G.P. Halada, Decontamination of uranium-contaminated steel surfaces by hydroxycarboxylic acid with uranium recovery, Environ. Sci. Technol. 39(13) (2005) 5015-5021.
[21] S. Kim, W.M. Bender, U. Becker, Exploring the kinetics of actinyl-EDTA reduction by ferrous iron using quantum-mechanical calculations, Phys. Chem. Chem. Phys. 23(9) (2021) 5298-5314.
[22] O. Gremy, D. Laurent, S. Coudert, N.M. Griffiths, L. Miccoli, Decorporation of Pu/Am actinides by chelation therapy: new arguments in favor of an intracellular component of DTPA action, Radiat. Res. 185(6) (2016) 568-579.
[23] A. Bhattacharyya, P.K. Mohapatra, Separation of trivalent actinides and lanthanides using various 'N', 'S' and mixed 'N,O' donor ligands: a review, Radiochim. Acta 107(9-11) (2019) 931-949.
[24] P. Thakur, J.L. Conca, L.J. Van De Burgt, G.R. Choppin, Complexation and the laser luminescence studies of Eu(III), Am(III), and Cm(III) with EDTA, CDTA, and PDTA and their ternary complexation with dicarboxylates, J. Coord. Chem. 62(23) (2009) 3719-3737.

[25] S.O. Bondareva, L.V. Spirikhin, A.N. Lobov, Y.I. Murinov, Solvent extraction of Neodymium(III) from chloride solutions using a mixture of diacylated diethylenetriamines and carboxylic acids, Solvent Extr. Ion Exch. 35(5) (2017) 332-344.
[26] H. Kitano, Y. Onishi, A. Kirishima, N. Sato, O. Tochiyama, Determination of the thermodynamic quantities of complexation between Eu(III) and carboxylic acids by microcalorimetry, Radiochim. Acta 94(9-11) (2006) 541-547.
[27] Z.R. Jones, M.Y. Livshits, F.D. White, E. Dalodiere, M.G. Ferrier, L.M. Lilley, K.E. Knope, S.A. Kozimor, V. Mocko, B.L. Scott, B.W. Stein, J.N. Wacker, D.H. Woen, Advancing understanding of actinide(iii) (Ac, Am, Cm) aqueous complexation chemistry, Chem. Sci. 12(15) (2021) 5638-5654.
[28] M.P. Jensen, K.L. Nash, Thermodynamics of dioxoneptunium(V) complexation by dicarboxylic acids, Radiochim. Acta 89(9) (2001) 557-564.
[29] T. Toraishi, I. Farkas, Z. Szabo, I. Grenthe, Complexation of Th(IV) and various lanthanides(III) by glycolic acid; potentiometric, C-13-NMR and EXAFS studies, J. Chem. Soc.-Dalton Trans. (20) (2002) 3805-3812.
[30] M.A. Brown, A.J. Kropf, A. Paulenova, A.V. Gelis, Aqueous complexation of citrate with neodymium(III) and americium(III): a study by potentiometry, absorption spectrophotometry, microcalorimetry, and XAFS, Dalton Trans. 43(17) (2014) 6446-6454.
[31] J.M. Monsallier, G.R. Choppin, Influence of humic acid size on actinide complexation, Radiochim. Acta 91(3) (2003) 135-139.
[32] M. Morgenstern, R. Klenze, J.I. Kim, The formation of mixed-hydroxo complexes of Cm(III) and Am(III) with humic acid in the neutral pH range, Radiochim. Acta 88(1) (2000) 7-16.
[33] C. Franz, G. Herrmann, N. Trautmann, Complexation of samarium(III) and americium(III) with humic acid at very low metal concentrations, Radiochim. Acta 77(3) (1997) 177-181.
[34] P.G. Jaison, P. Kumar, V.M. Telmore, S.K. Aggarwal, Electrospray ionization mass spectrometric studies on uranyl complex with alpha-hydroxyisobutyric acid in water-methanol medium, Rapid Commun. Mass Spectrom. 27(10) (2013) 1105-1118.
[35] Y.J. Zhang, N.D. Bryan, F.R. Livens, M.N. Jones, Selectivity in the complexation of actinides by humic substances, Environ. Pollut. 96(3) (1997) 361-367.
[36] G.R. Choppin, N. LabonneWall, Comparison of two models for metal-humic interactions, J. Radioanal. Nucl. Chem. 221(1-2) (1997) 67-71.
[37] P.E. Reiller, N.D.M. Evans, G. Szabo, Complexation parameters for the actinides(IV)-humic acid system: a search for consistency and application to laboratory and field observations, Radiochim. Acta 96(6) (2008) 345-358.

[38] K. Schmeide, T. Reich, S. Sachs, G. Bernhard, Plutonium(III) complexation by humic substances studied by X-ray absorption fine structure spectroscopy, Inorg. Chim. Acta 359(1) (2006) 237-242.
[39] T. Sakuragi, S. Sawa, S. Sato, T. Kozaki, T. Mitsugashira, M. Hara, Y. Suzuki, Interaction of americium(III) with humic acid over wide pH region, J. Radioanal. Nucl. Chem. 265(3) (2005) 349-353.
[40] V. Beaugeard, J. Muller, A. Graillot, X.Y. Ding, J.J. Robin, S. Monge, Acidic polymeric sorbents for the removal of metallic pollution in water: A review, React. Funct. Polym. 152 (2020) 104599.
[41] X.F. Yi, Z.Q. Xu, Y. Liu, X.Y. Guo, M.R. Ou, X.P. Xu, Highly efficient removal of uranium(VI) from wastewater by polyacrylic acid hydrogels, RSC Adv. 7(11) (2017) 6278-6287.
[42] D.R. Frohlich, P.J. Panak, The complexation of Eu(III) and Cm(III) with polyacrylate as a model compound for complex polycarboxylates studied by laser fluorescence spectroscopy, J. Lumines. 212 (2019) 166-170.
[43] S.Z. Ahammad, J. Gomes, T.R. Sreekrishnan, Wastewater treatment for production of H2S-free biogas, Journal of Chemical Technology and Biotechnology 83(8) (2008) 1163-1169.
[44] F. ArnaudNeu, S. Cremin, S. Harris, M.A. McKervey, M.J. SchwingWeill, P. Schwinte, A. Walker, Complexation of Pr3+, Eu3+, Yb3+ and Th4+ ions by calixarene carboxylates, J. Chem. Soc.-Dalton Trans. (3) (1997) 329-334.
[45] H. Kweon, M.K. Yoo, I.K. Park, T.H. Kim, H.C. Lee, H.S. Lee, J.S. Oh, T. Akaike, C.S. Cho, A novel degradable polycaprolactone networks for tissue engineering, Biomaterials 24(5) (2003) 801-808.
[46] M.H. Huang, S.M. Li, D.W. Hutmacher, J.T. Schantz, C.A. Vacanti, C. Braud, M. Vert, Degradation and cell culture studies on block copolymers prepared by ring opening polymerization of epsilon-caprolactone in the presence of poly(ethylene glycol), J. Biomed. Mater. Res. Part A 69A(3) (2004) 417-427.
[47] E. Bayer, W. Rapp, Polystyrene-immobilized PEG chains, in: J.M. Harris (Ed.), Poly(Ethylene Glycol) Chemistry, Springer US1992, pp. 325-345.
[48] N. Das, Preparation methods and properties of hydrogel: a review, International Journal of Pharmacy and Pharmaceutical Sciences 5(3) (2013) 112-117.
[49] C.Y. Gong, S.A. Shi, L. Wu, M.L. Gou, Q.Q. Yin, Q.F. Guo, P.W. Dong, F. Zhang, F. Luo, X. Zhao, Y.Q. Wei, Z.Y. Qian, Biodegradable in situ gel-forming controlled drug delivery system based on thermosensitive PCL-PEG-PCL hydrogel. Part 2: Sol-gel-sol transition and drug delivery behavior, Acta Biomater. 5(9) (2009) 3358-3370.

[50] M.H. Perez, C. Zinutti, A. Lamprecht, N. Ubrich, A. Astier, M. Hoffman, R. Bodmeier, P. Maincent, The preparation and evaluation of poly(epsilon-caprolactone) microparticles containing both a lipophilic and a hydrophilic drug, J. Control. Release 65(3) (2000) 429-438.
[51] H.Z. Deng, A.J. Dong, J.B. Song, X.Y. Chen, Injectable thermosensitive hydrogel systems based on functional PEG/PCL block polymer for local drug delivery, J. Control. Release 297 (2019) 60-70.
[52] B.S. Makhmalzadeh, O. Molavi, M.R. Vakili, H.F. Zhang, A. Solimani, H.S. Abyaneh, R. Loebenberg, R. Lai, A. Lavasanifar, Functionalized caprolactone-polyethylene glycol based thermo-responsive hydrogels of silibinin for the treatment of malignant melanoma, J. Pharm. Pharm. Sci. 21 (2018) 143-159.
[53] A.M. Master, M.E. Rodriguez, M.E. Kenney, N.L. Oleinick, A. Sen Gupta, Delivery of the photosensitizer Pc 4 in PEG-PCL micelles for In vitro PDT studies, J. Pharm. Sci. 99(5) (2010) 2386-2398.
[54] S. Saghebasl, S. Davaran, R. Rahbarghazi, A. Montaseri, R. Salehi, A. Ramazani, Synthesis and in vitro evaluation of thermosensitive hydrogel scaffolds based on (PNIPAAm-PCL-PEG-PCL-PNIPAAm)/Gelatin and (PCL-PEG-PCL)/Gelatin for use in cartilage tissue engineering, Journal of Biomaterials Science Polymer Edition 29(10) (2018) 1185-1206.
[55] A. Mahmud, X.B. Xiong, A. Lavasanifar, Novel self-associating poly(ethylene oxide)-block-poly(epsilon-caprolactone) block copolymers with functional side groups on the polyester block for drug delivery, Macromolecules 39(26) (2006) 9419-9428.
[56] M. Sriyai, T. Chaiwon, R. Molloy, P. Meepowpan, W. Punyodom, Efficiency of liquid tin(ii) n-alkoxide initiators in the ring-opening polymerization of l-lactide: kinetic studies by non-isothermal differential scanning calorimetry, RSC Adv. 10(71) (2020) 43566-43578.
[57] A.C. Albertsson, I.K. Varma, Aliphatic polyesters: Synthesis, properties and applications, in: A.C. Albertsson (Ed.), Degradable Aliphatic Polyesters2002, pp. 1-40.
[58] E. Freire, Isothermal titration calorimetry: controlling binding forces in lead optimization, Drug Discovery Today. Technologies 1(3) (2004) 295-299.
[59] T. Christensen, D.M. Gooden, J.E. Kung, E.J. Toone, Additivity and the physical basis of multivalency effects: a thermodynamic investigation of the calcium EDTA interaction, J. Am. Chem. Soc. 125(24) (2003) 7357-7366.
[60] D.E. Wilcox, Isothermal titration calorimetry of metal ions binding to proteins: an overview of recent studies, Inorg. Chim. Acta 361(4) (2008) 857-867.
[61] V. Karlsen, E.B. Heggset, M. Sorlie, The use of isothermal titration calorimetry to determine the thermodynamics of metal ion binding to low-cost sorbents, Thermochim. Acta 501(1-2) (2010) 119-121.

[62] P. Zanonato, P. Di Bernardo, A. Bismondo, L.F. Rao, G.R. Choppin, Thermodynamic studies of the complexation between neodymium and acetate at elevated temperatures, J. Solut. Chem. 30(1) (2001) 1-18.
[63] P.R. Zalupski, K.L. Nash, L.R. Martin, Thermodynamic features of the complexation of Neodymium(III) and Americium(III) by lactate in trifluoromethanesulfonate media, J. Solut. Chem. 39(8) (2010) 1213-1229.
[64] Z.C. Zhang, B. Bottenus, S.B. Clark, G.X. Tian, P. Zanonato, L.F. Rao, Complexation of gluconic acid with Nd(III) in acidic solutions: a thermodynamic study, J. Alloy. Compd. 444 (2007) 470-476.
[65] V.K. Manchanda, P.K. Mohapatra, C.Y. Zhu, R.M. Izatt, Thermodynamics of the complexation of Cerium(III), Europium(III), and Erbium(III) with 1,4,10-trioxa-7,13-diazapentadecane-N,N'-diacetic acid and 1,4,10,13-tetraoxa-7,16-diazaoxacyclooctadecane-N,N'-diacetic acid, Journal of the Chemical Society Dalton Transactions (10) (1995) 1583-1585.
[66] R.R. Samal, M. Mishra, U. Subudhi, Differential interaction of cerium chloride with bovine liver catalase: a computational and biophysical study, Chemosphere 239 (2020) 124769.
[67] M.J. Sanchez-Fernandez, M.R. Immers, R.P.F. Lanao, F. Yang, J. Bender, J. Mecinovic, S.C.G. Leeuwenburgh, J.C.M. van Hest, Alendronate-functionalized poly(2-oxazoline)s with tunable affinity for calcium cations, Biomacromolecules 20(8) (2019) 2913-2921.
[68] J.W. Steed, J.L. Atwood, Supramolecular Chemistry, Wiley2013.
[69] F.S. Teodoro, S.N.D. Ramos, M.M.C. Elias, A.B. Mageste, G.M.D. Ferreira, L.H.M. da Silva, L.F. Gil, L.V.A. Gurgel, Synthesis and application of a new carboxylated cellulose derivative. Part I: removal of Co2+, Cu2+ and Ni2+ from monocomponent spiked aqueous solution, J. Colloid Interface Sci. 483 (2016) 185-200.
[70] V.O. Vasylechko, E.T. Stechynska, O.D. Stashkiv, G.V. Gryshchouk, I.O. Patsay, Sorption of neodymium and gadolinium on transcarpathian clinoptilolite, Acta Phys. Pol. A 133(4) (2018) 794-797.
[71] J. Ponou, L.P. Wang, G. Dodbiba, K. Okaya, T. Fujita, K. Mitsuhashi, T. Atarashi, G. Satoh, M. Noda, Recovery of rare earth elements from aqueous solution obtained from vietnamese clay minerals using dried and carbonized parachlorella, Journal of Environmental Chemical Engineering 2(2) (2014) 1070-1081.
[72] A.A. Naser, G.E.S. El-Deen, A.A. Bhran, S.S. Metwally, A.M. El-Kamash, Elaboration of impregnated composite for sorption of Europium and Neodymium ions from aqueous solutions, J. Ind. Eng. Chem. 32 (2015) 264-272.
[73] W.R. Mohamed, S.S. Metwally, H.A. Ibrahim, E.A. El-Sherief, H.S. Mekhamer, I.M.I. Moustafa, E.M. Mabrouk, Impregnation of task-specific ionic liquid into a solid support for

removal of neodymium and gadolinium ions from aqueous solution, J. Mol. Liq. 236 (2017) 9-17.
[74] T. Ogata, H. Narita, M. Tanaka, Adsorption behavior of rare earth elements on silica gel modified with diglycol amic acid, Hydrometallurgy 152 (2015) 178-182.
[75] H. Demey, B. Lapo, M. Ruiz, A. Fortuny, M. Marchand, A.M. Sastre, Neodymium recovery by Chitosan/Iron(III) hydroxide ChiFer(III) sorbent material: batch and column systems, Polymers 10(2) (2018) 204.
[76] A. Vlachou, B.D. Symeopoulos, A.A. Koutinas, A comparative study of neodymium sorption by yeast cells, Radiochim. Acta 97(8) (2009) 437-441.
[77] C. Gok, Neodymium and samarium recovery by magnetic nano-hydroxyapatite, J. Radioanal. Nucl. Chem. 301(3) (2014) 641-651.
[78] S. Sert, C. Kutahyali, S. Inan, Z. Talip, B. Cetinkaya, M. Eral, Biosorption of lanthanum and cerium from aqueous solutions by platanus orientalis leaf powder, Hydrometallurgy 90(1) (2008) 13-18.
[79] W.R. Archer, A. Fiorito, S.L. Heinz-Kunert, P.L. MacNicol, S.A. Winn, M.D. Schulz, Synthesis and Rare-Earth-Element Chelation Properties of Linear Poly(ethylenimine methylenephosphonate), Macromolecules 53(6) (2020) 2061-2068.
[80] M.R. Awual, T. Yaita, H. Shiwaku, Design a novel optical adsorbent for simultaneous ultra-trace cerium(III) detection, sorption and recovery, Chem. Eng. J. 228 (2013) 327-335.
[81] D. Sofronov, A. Krasnopyorova, N. Efimova, A. Oreshina, E. Bryleva, G. Yuhno, S. Lavrynenko, M. Rucki, Extraction of radionuclides of cerium, europium, cobalt and strontium with Mn3O4, MnO2, and MNOOH sorbents, Process Saf. Environ. Protect. 125 (2019) 157-163.
[82] I.M. Ahmed, R. Gamal, A.A. Helal, S.A. Abo-El-Enein, A.A. Helal, Kinetic sorption study of Cerium (IV) on magnetite nanoparticles, Part. Sci. Technol. 35(6) (2017) 643-652.
[83] D. Sadovsky, A. Brenner, B. Astrachan, B. Asaf, R. Gonen, Biosorption potential of cerium ions using spirulina biomass, J. Rare Earths 34(6) (2016) 644-652.
[84] V.K. Jain, A. Handa, S.S. Sait, P. Shrivastav, Y.K. Agrawal, Pre-concentration, separation and trace determination of lanthanum(III), cerium(III), thorium(IV) and uranium(VI) on polymer supported o-vanillinsemicarbazone, Anal. Chim. Acta 429(2) (2001) 237-246.